The International Journal of Advanced Manufacturing Technology (2022) 120:4147–4157
https://doi.org/10.1007/s00170-022-09007-4

ORIGINAL ARTICLE

Simulation and experimental researches on multi-plate rubber pad forming of two-step micro-channel based on different forming driving models

Teng Fei[1] · Wang Hongyu[1] · Shi Shengnan[1] · Jiang Lei[1] · Sun Juncai[1] · Sun Jie[2] · Di Hongshuang[2] · Zhang Shunhu[3]

Received: 6 October 2021 / Accepted: 2 March 2022 / Published online: 14 March 2022

Abstract
Surface micro-channels with different structures have a variety of functions. In order to further develop these functions, micro-channel design and forming process are constantly being innovated. In this paper, the advanced rubber pad forming technology is used to manufacture the new two-step micro-channel structure. Forced convection can be caused by this kind of micro-channel in three dimensions of the gas, which can reduce the flow rate and make the gas evenly distributed. Therefore, it can be used in bipolar plates of PEMFC (proton exchange membrane fuel cell). According to the driving mode, forming mode is divided into active forming and passive forming. The metal plates formed in these ways are studied, and the advantages and differences of forming results are discussed. The 304 stainless steel sheet with the thickness of 0.1 mm is used in the manufacturing process. Polyurethane with shore A70 hardness and 60 mm total thickness is selected as rubber pad. And then, two models of forming two metal plates simultaneously in one time are presented. In order to verify the accuracy of the model, finite element method and forming experiment are carried out. It is shown that the rubber pad forming process is a feasible process for producing multiple two-step micro-channel metal plates in one time.

Keywords Rubber pad forming · Finite element method · Micro-channel · Active forming

1 Introduction

In recent years, due to the miniaturization of microsystem technology, the demand for micro sheet metal components has been increased [1]. At the same time, it is worth mentioning that the forming accuracy, shape, surface quality, and low cost are considered indispensable requirements. Rubber pad forming, based on the characteristics of high precision, high surface quality, and low cost, has the potential to manufacture complex shape parts [2, 3]. As shown in Fig. 1, plate is placed on the rubber pad. Then the mold is pressed down the plate and the rubber pad simultaneously [4]. Only one rigid mold is required, and polyurethane rubber can be reused, so the production cost of the mold is greatly reduced. Because hydrostatic pressure is applied to the material, the plate is easy to be machined. Excellent surface quality with no tool marks can be formed by using rubber pad as a flexible die [5]. Due to the rubber pad, the problem of inconsistent fit between upper and lower molds in stamping process is avoided. Assembly difficulty is reduced, and multiple processes can be combined. Because of the low melting point of polyurethane rubber, this technology is suitable for the production of micro metal sheet at room temperature [6].

Many studies have been carried out to demonstrate that the forming of micro metal sheet can be influenced by the relevant process parameters. Lee et al. [7] optimized rubber pad forming process to form aluminum plates. It is proposed that the size parameters can affect the forming results. Wang et al. [8] used rubber pad forming process to form pure nickel plate. They mentioned that the forming depth was related to the thickness of the plate. Gau et al. [9] indicated that specimens with lower thickness to depth ratio had better formability in rubber pad forming. Wang et al.

✉ Wang Hongyu
wanghongyusci@yeah.net

1 Transportation Engineering College, Dalian Maritime University, No. 1 Linghai Road, Ganjingzi District, Dalian, Liaoning 106026, People's Republic of China

2 State Key Laboratory of Rolling & Automation, Northeastern University, Shenyang, Liaoning 110819, People's Republic of China

3 Shagang School of Iron and Steel, Soochow University, Suzhou 215002, People's Republic of China

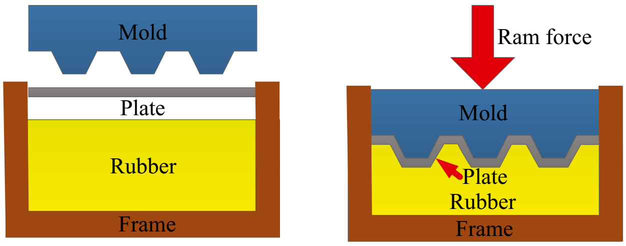

Fig. 1 Schematic of rubber pad forming process

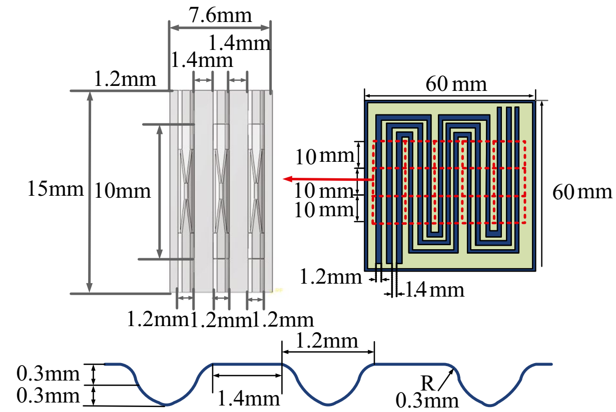

Fig. 2 Dimension parameters of two-step micro-channel

[10, 11] reported that the micro-channel could be formed on 304 annealed stainless steel using rubber pad forming. They also suggested that forming results is determined by the size parameters of the micro-channel. Because the plate used in the stamping process is very thin, thin to 0.1 mm, there is a problem of irregular flatness due to deformation, after forming is done. It will be crumpled and broken at the micro-channel curvature. Jin et al. [12] found that these problems in stamping can be solved by using the rubber pad forming. Hossein et al. [13] obtained the experimental results of the micro-channel of stainless steel 316 bipolar plates. It is shown that difference of forming results can be caused by the draft angles and the corner radius of the micro-channel. These studies, however, have only focused on simple straight channels. Therefore, in order to form products with complicated shapes, more experimental data are needed.

With the development of micro-channel technology, it is found that micro-channels with unique structures have unique functions, for example, heat dissipation [14], drag reduction [15], super hydrophobic [16], etc. Micro-channels are often used in fuel cell bipolar plates because of their ability to direct gas flow [17]. Li et al. [18] designed a novel three-dimensional micro-channel. It is also known as two-step micro-channel. Due to the periodic wavy structure of the micro-channel, the gas is forced to convection during the flow. Gas flow rate is reduced, allowing more time for the reaction and improving battery performance. However, the researches on this new micro-channel are more focused on the property, but the forming process is rarely studied. Teng et al. [19] used the slab method and FEM (finite

Fig. 3 Four rubber pad forming process models

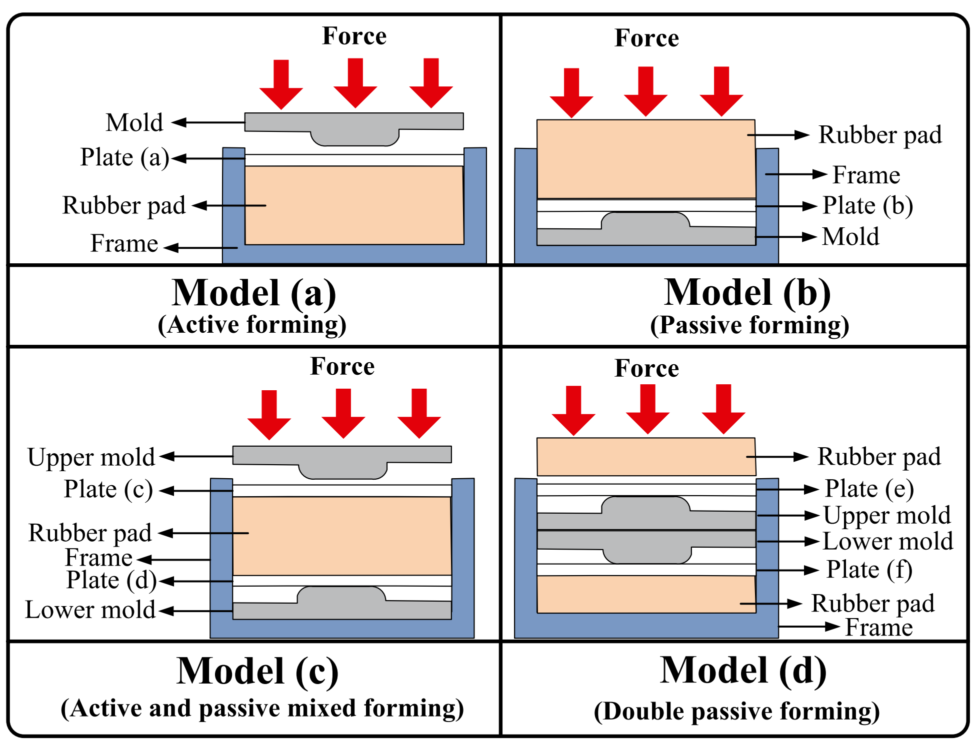

element modeling) to study the forming process of two-step micro-channels in rubber pad forming process. Through analysis, it is suggested that when polyurethane rubber is used as a punch, the plates tend to be less prone to stress concentration. The flatness of the plate is higher, and the surface scratches are less. However, at the same time, it is also proposed that the shape of the second-step structure has a decisive influence on the formability of the micro-channel. Therefore, as shown in Fig. 2, the two-step micro-channel structure which is easy to be formed is determined. This structure is also used in this study. However, the above studies are limited to the research of structure, and the forming of entire plate with two-step micro-channel is still rarely studied.

This study aims to determine the feasibility of forming this fresh micro-channel in rubber pad forming. As shown in Fig. 3, four different rubber pad forming models are established in this paper. The forming process can be divided into active forming and passive forming according to the different force transfer medium. As shown in models (a) and (b), active forming is defined when pressure is applied directly to the plate through mold, while passive forming is defined when pressure is applied to the plate through rubber pad. And then, as shown in models (c) and (d), it is proposed that two metal sheets can be formed simultaneously in one deep drawing cycle. According to the different force transfer medium, the two models are named active and passive mixed forming and double passive forming, respectively. In addition, the plates manufactured by different models are named separately as shown in Table 1. In this paper, the finite element simulation and deep drawing experiment are used to analyze this process. The difference between active forming and passive forming is compared and studied. The feasibility of forming two plates at the same time is discussed. Four different models were evaluated comprehensively based on the analytical results of finite element simulation and forming experiment. The new method of rubber pad forming process proposed in this study will inform future work.

Table 1 Plates manufactured by different models

Model	Forming process	Sample
Model (a)	Active forming	Plate (a)
Model (b)	Passive forming	Plate (b)
Model (c)	Active and passive mixed forming	Plate (c) (formed by active forming) Plate (d) (formed by passive forming)
Model (d)	Dual-passive forming	Plate (e) (formed by upper mold) Plate (f) (formed by lower mold)

2 Finite element model

In order to simulate this process, Abaqus CAE software is used in this study. As shown in Fig. 4, four different models are built. All finite element models consist of three components: rubber pad, plate, and rigid mold. To simplify the

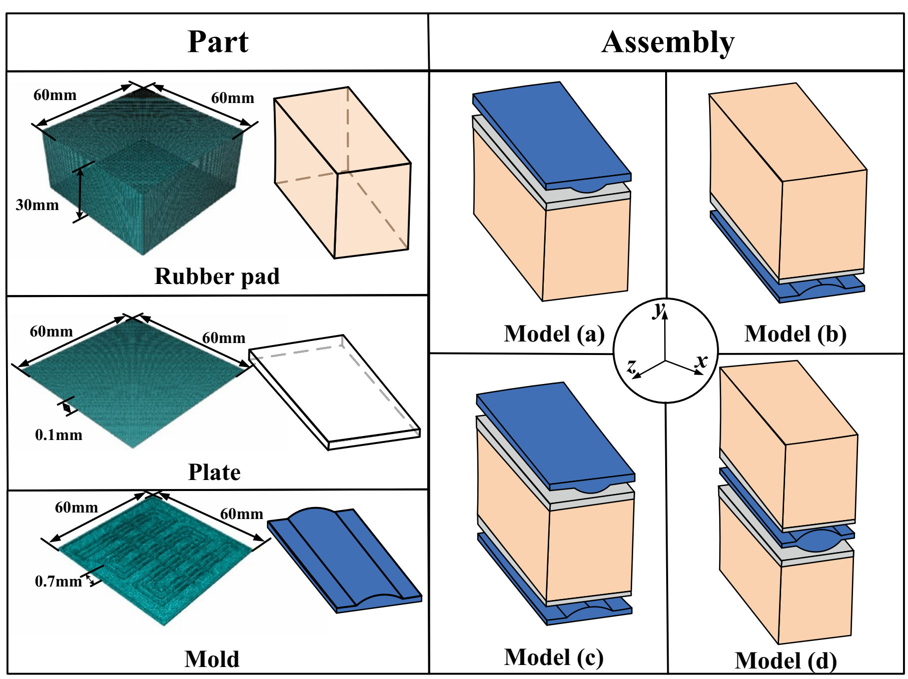

Fig. 4 Modeling and meshing as well as the assembling of rubber pad forming simulation

Table 2 Chemical composition list of SS304 (wt%)

	C	Si	Mn	P	S	Cr	Ni	Fe
SS304	≤ 0.08	≤ 0.1	≤ 0.2	≤ 0.045	≤ 0.03	18.00 ~ 20.00	8.00 ~ 10.50	Balance

model, the frame is omitted in the simulation. The displacements of rubber pads are limited by applying proper boundary conditions on its surfaces. The only free surfaces of the rubber pads are those in contact with plates. Rigid molds are defined as rigid parts, so no material properties are specified. Both plates and rubber pads are modeled as deformable elements. The plastic behavior of plate is assumed to be isotropic. Stainless steel 304 (SS304) was chosen as the original material of the plate with a thickness of 0.1 mm. The density, Young's modulus, and Poisson's ratio of SS304 are 7.833 g/cm^3, 162.5 GPa, and 0.3, respectively. [20, 21] The following formula can satisfy the plastic stress-strain relationship: $\sigma = 1421(0.047 + \varepsilon)^{0.561}$. The unit of $\boldsymbol{\sigma}$ is Pa, and the unit of $\boldsymbol{\varepsilon}$ is mm. In this study, polyurethane rubber with a hardness of 70A (HD70) is used as rubber pad. The Mooney-Rivlin model is used to describe the incompressible and nonlinear hyper-elastic behavior of rubber material. In this model, only two parameters ($\boldsymbol{C_{10}}$ and $\boldsymbol{C_{01}}$) are considered. Their values are 0.736 and 0.184, respectively [22].

2.1 Finite element mesh

In the finite element analysis of two-step micro-channel, the rigid molds are defined as analytical rigid body. At the same time, plates and rubber pads are modeled as deformable bodies. Their mesh types are C3D8RH and C3D8R, respectively. The hybrid element is incompressible and is suitable for rubber-like materials [23].

2.2 Dynamic contact conditions

In the simulation of rubber pad forming process, there are two different contact pairs between plate, rubber pad, and rigid mold. One is the contact surface between rigid mold and plate, the other one is the contact surface between plate and rubber pad. The penalty solution method is adopted for both contact pairs, and the friction behavior of each contact pair is assumed to follow Coulomb's model. By this method, the critical shear stress is eliminated by Coulomb's friction model on the basis of contact normal pressure [24]. The friction coefficient between the rigid mold and the plate is 0.1, and that between the plate or mold and the rubber pad is 0.2.

2.3 Loading and boundary conditions

As shown in Fig. 3, the rubber pads are confined to the frame. To simplify the model, constraints were added to the rubber pads to simulate the role of the frame. In passive forming, molds are fixed in all directions. The rubber pad is set to move only in the vertical direction. In active forming, molds are fixed in the horizontal direction and are allowed to move only in the vertical direction. The displacement of the mold is controlled by displacement/rotation.

3 Experimental setup and methodology

In order to further study the process of rubber pad forming two metal sheets in one pass, the deep drawing experiments were also carried out. The steel plate is annealed SS304 with a thickness of 0.1 mm, and its chemical composition is shown in Table 2. The sheet metal is pretreated before forming. The plates are cut to the same size of 60 mm × 60 mm. To get better formability, they were held for 3 or 5 min at 1010–1120 ℃ and then cooled to room temperature in a box-type furnace.

During the forming experiment, the plates were formed under a load of 50 kN. The extrusion speed is 0.5 mm/s. The molds are made of Cr12MoV. After heat treatment, the hardness can reach 55 ~ 60 HRC. The chemical composition of mold is shown in Table 3.

As shown in Fig. 5, the experiment was carried out on a press machine with a clamp. The frame is assembled in the clamp. The whole device is composed of four parts: frame, metal mold, rubber pad, and metal plate. The rubber pad forming process is preserved in the frame. The function of the frame is to limit the deformation of the rubber pad in the horizontal direction. In this way, all deformation of the rubber pad will be limited to the vertical direction. The setting of the rubber pad in the experiment is the same as in the finite element simulation. The elastic

Table 3 Chemical composition list of $Cr_{12}MoV$ (wt%)

	C	Si	Mn	Cr	Mo	V	P	Fe
$Cr_{12}MoV$	1.49	0.27	0.26	11.65	0.48	0.22	≤ 0.03	Balance

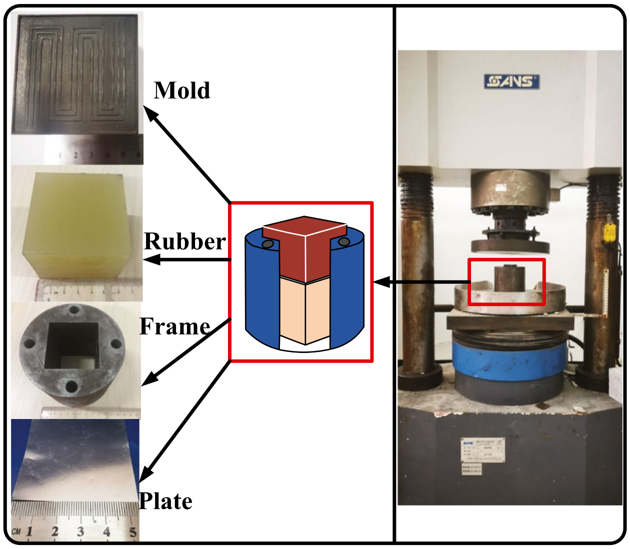

Fig. 5 Forming experiment

deformation of the rubber pad along vertical direction could be used to take part in the forming process. The plate is placed between the mold and the rubber pad so that it can be extruded into designed shape under pressure. The total height of mold, plate, and rubber pad is slightly higher than that of the frame. When the punch of the press machine is moved down, the plate can be formed into the shape of mold. The size of the rubber pad is 60 mm × 60 mm. In order to ensure the consistency of each model, the total height of the rubber pad has been kept at 60 mm. The size of the plate is 60 mm × 60 mm × 0.1 mm. The size of the mold is 60 mm × 60 mm × 50 mm. The height of the two-step micro-channel in the mold is 0.56 mm. The mold is precisely machined using a numerical control machine. The actual forming process is similar to the FEM process. The shapes of the molds are made according to the parameters in Fig. 2. In the process of rubber pad forming, one side of the mold is replaced by polyurethane rubber, and the other side is a convex metal mold. Macroscopic and microscopic photos of the micro-channels are shown below. The results of deep drawing experiments are discussed.

4 Results and discussion

4.1 Finite element analysis

According to the finite element results, the results of forming a single plate using rubber pad forming process are discussed. The forming process can be divided into active forming and passive forming according to the different force transmission medium. The displacement nephogram and stress nephogram after active forming and passive forming are shown in Fig. 6. It can be clearly seen that the micro-channels are clearly formed on the plate in both forms. The stress on the plate is described by contour. When active forming is used, the stress of plate is larger and more uniform, and the deformation is more sufficient. Micro-channels can be formed accurately and smoothly. If passive forming is used, the stress shown in the plate is reduced because the stress is not applied directly by the punch. As a result, the forming results of micro-channels become worse.

The process of forming two metal plates simultaneously by active and passive mixed forming is studied. As shown in Fig. 7, in the finite element simulation, both plates are accurately formed into the designed shape. The stress distribution of sheet metal in the forming process is shown. In the active and passive mixed forming process, the stress of the two plates is almost the same, and both are sufficient. Because both plates are subjected to sufficient stress, the micro-channels on them can be accurately and smoothly formed. This can be interpreted that when an external force is applied to polyurethane rubber, the stress generated by the elastic deformation can be evenly transmitted to its upper and lower surfaces, where the plates are tightly connected. Next, the plates are formed.

Fig. 6 Finite element simulation results of plates (**a**) and (**b**)

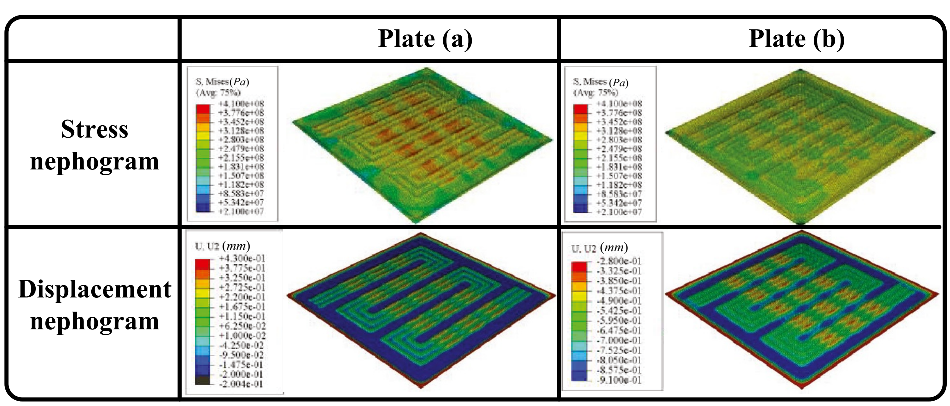

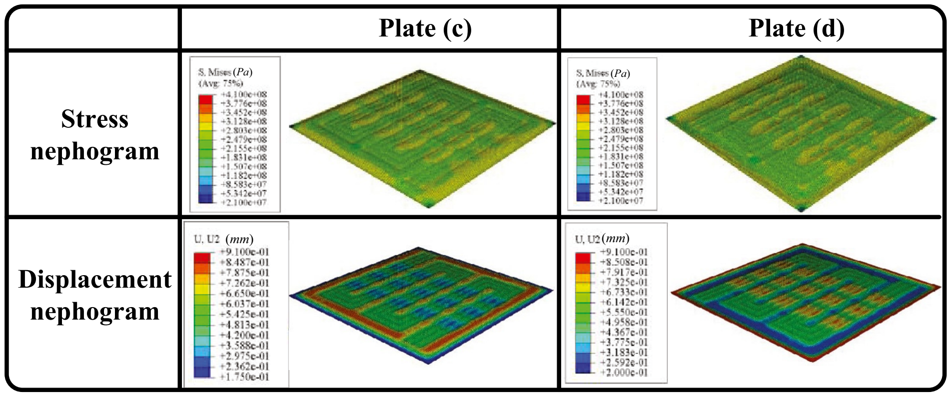

Fig. 7 Finite element simulation results of plates (**c**) and (**d**)

The process of forming two metal sheets simultaneously by double passive forming is studied. As shown in Fig. 8, the micro-channels on both plates are clearly formed. However, the depth and accuracy of the forming are somewhat lacking. According to the stress distribution in the forming process, it can be found that in the double passive forming process, the stress of the two plates is almost the same, but compared with the active and passive mixed forming, the stress of the plates is obviously reduced. The forming depth of the micro-channel is affected because there is not enough stress on either plate. This means that if the pressure of the punch cannot be applied directly to the plate, relying only on the elastic deformation of the rubber, the sheet metal will be difficult to form into the designed shape.

4.2 Forming profile and forming depth

In order to verify the accuracy of finite element analysis, the two-step micro-channel metal sheet was formed by deep drawing experiment. As shown in Fig. 9, some samples of the plate after forming are shown. The plate is then cut in the vertical direction of the two-step micro-channel as observed in Fig. 10. The forming results of samples formed by each model are discussed separately.

As shown by the red-dotted line in Fig. 9, the forming plates were cut along the top of the second-step structure of the straight micro-channel, and their filling contour was studied. As shown in Fig. 10, the segmented sample was then installed. The surface is polished to accurately measure the profile of the sample under the microscope. First, a VMMVMS measuring device was used for observation at × 2 magnification. Subsequently, in order to obtain higher accuracy, × 4 magnification optical microscope was used. Using measurement software connected to the computer system and attached to the microscope, the filled profile of the channel is obtained.

The morphologies of the micro-channels were observed by magnifying them with an optical microscope. The depth and profile of the micro-channels are determined by the measuring software connected with the computer system and attached to the microscope.

The plate shown in Fig. 11a is manufactured by active forming method with a cross section perpendicular to the micro-channel. It can be found that the depth of each micro-channel is relatively uniform. The depth of the micro-channel is 0.502 mm (the design depth is 0.56 mm). As shown, the profile is clearly displayed. The red line is used to show the shape of the micro-channel, and the blue

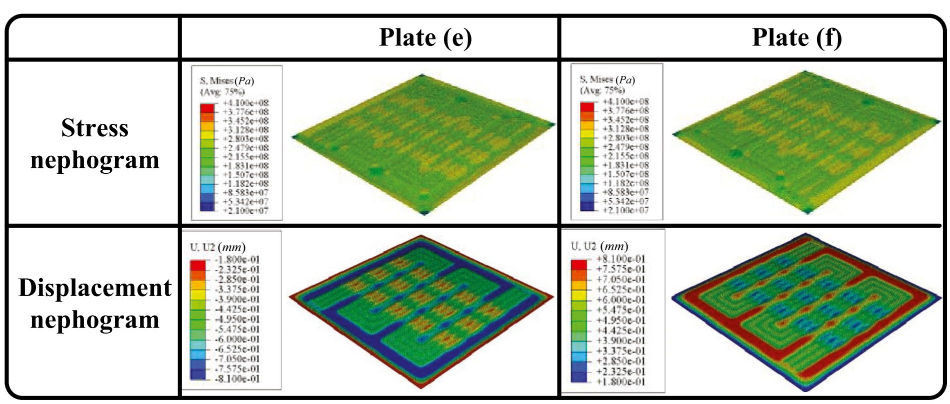

Fig. 8 Finite element simulation results of plate (**e**) and (**f**)

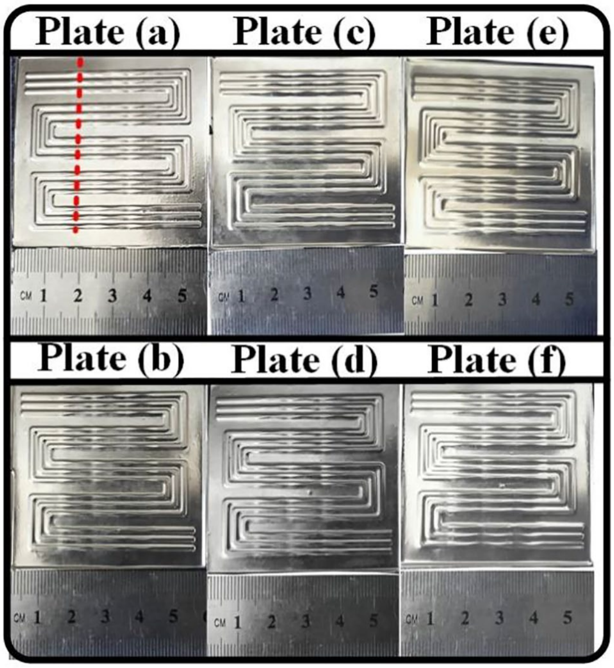

Fig. 9 Plates formed by different models

line is the shape of the designed. Through observation, it can be found that the sheet formed by active forming is basically consistent with the designed shape, and the depth and width have reached the designed size.

As shown in Fig. 11b, a plate produced by passive forming is shown in a cross section perpendicular to the micro-channel direction. The depth of each micro-channel is uniform. The depth of the micro-channel is 0.482 mm (the designed depth is 0.56 mm). As shown, the profile is clearly displayed. Through observation, it can be found that the plate formed by passive forming is basically consistent with the designed shape, but the forming depth and width are not up to the designed size.

The cross sections of two plates, perpendicular to the direction of the micro-channel, are shown in Fig. 12. Through observation, it can be found that the forming depths of each micro-channel of the two plates are relatively uniform. The actual depths of micro-channel reach 0.489 mm and 0.502 mm, respectively. As shown, the actual filling profile is clearly displayed. It can be found that the sheets formed by active forming and passive forming are both basically consistent with the designed depth and width. However, there is still an error between the formed shape and the designed shape, which may be caused by the springback after forming or the cutting method of the plate.

The cross sections of two plates, perpendicular to the direction of the micro-channel, are shown in Fig. 13. It can be found that the forming depths of each micro-channel of the two plates are small. The depths of micro-channels are only 0.414 mm and 0.393 mm, respectively. As shown, the actual filling profile is clearly displayed. Through observation, it can be found that although the two plates produced

Fig. 10 Microscopy images of two-step micro-channel

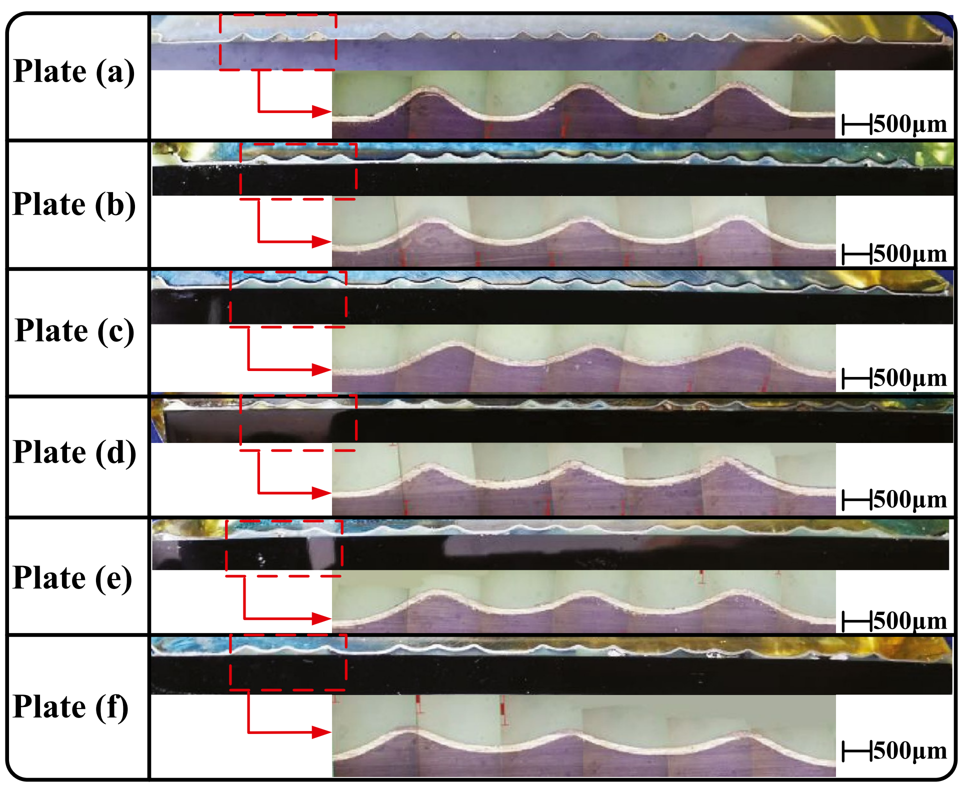

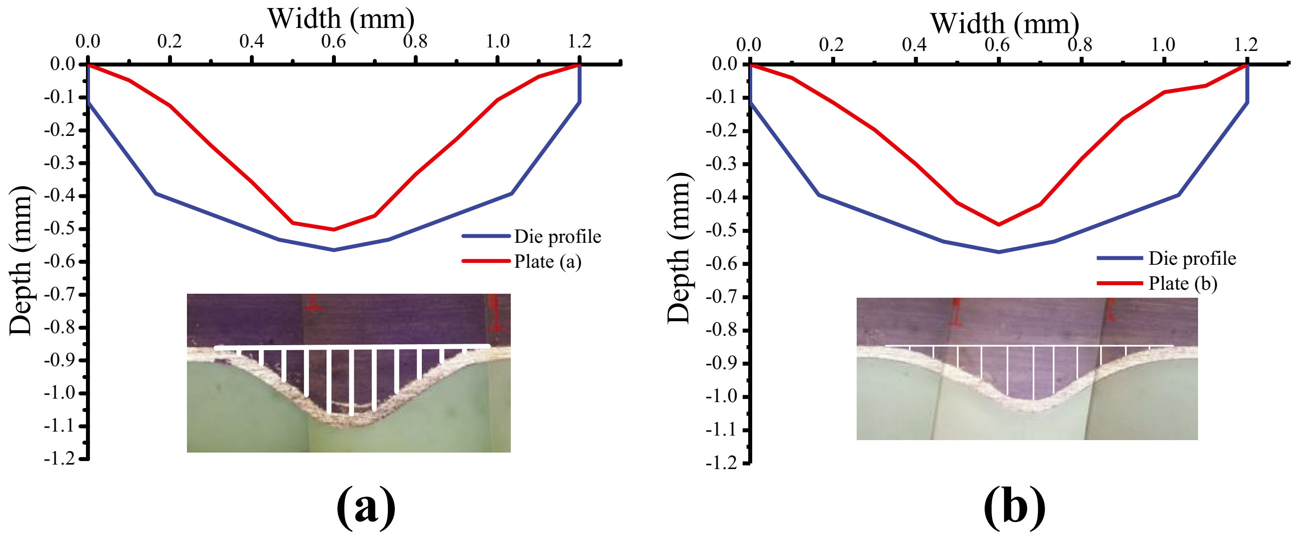

Fig. 11 Profile diagram of plates formed by models (a) and (b)

by the double passive forming method are formed into the designed shape, there is a large gap between the forming depth and the designed size.

4.3 Thickness distribution

Because the thickness distribution of each micro-channel is symmetric, it is possible to consider analyzing half of the micro-channel in the formed plate. As shown in Fig. 14, variation in thickness can be divided into three areas based on previous studies [19]. The thickness reduction in area A is very small. This is mainly because the plate does not satisfy the condition of yield criterion in this area, so there is no plastic deformation that occurs. This area should have a thickness similar to the initial thickness. In area B, thickness is rapidly reduced, and the thickness of the micro-channel is minimal in this area. This is due to the considerable stretching of the sheet during the forming process in the corner area. At the same time, the depth of the micro-channel is also increased, resulting in a lack of material feed in the area. In the second-step micro-channel area (area C), the thickness distribution tends to increase due to the decrease of tensile stress. Based on the above analysis, the thickness distribution of the metal sheet manufactured by this method is uniform.

The minimum thickness of each plate is shown in Fig. 15. It can be found that in active forming, the minimum thickness of the plate is 0.0847 mm, about 84.7% of the original

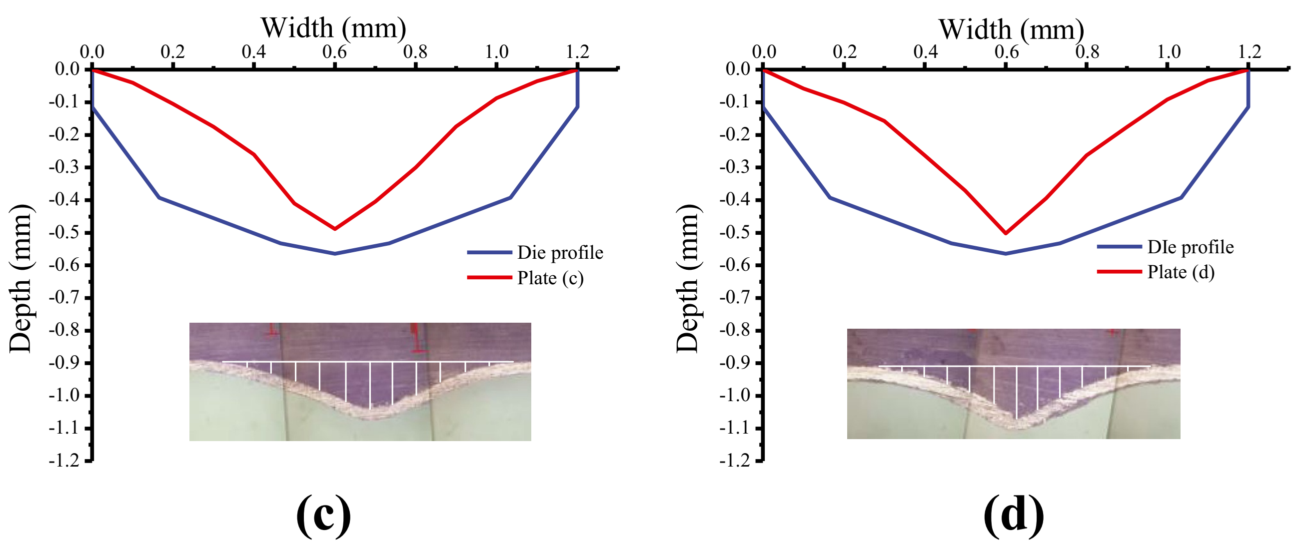

Fig. 12 Profile diagram of plates formed by model (c)

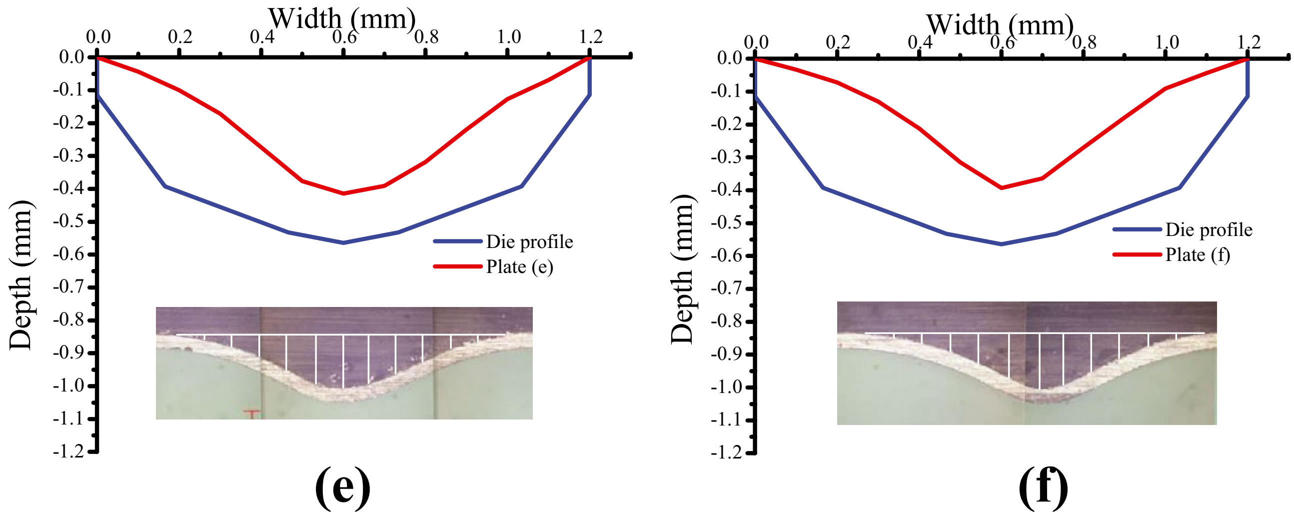

Fig. 13 Profile diagram of plates formed by model (d)

thickness. As a result of the larger stress, the thickness of the plate thinning degree is relatively larger. In passive forming, the minimum thickness of the plate is 0.0945 mm, approximately 94.5% of the original thickness. In active and passive mixed forming, the minimum thickness of the plates is 0.088 mm and 0.091 mm, accounting for 88% and 91% of the initial thickness, respectively. Due to the larger stress, plastic deformation can be full and uniform, so the thickness of the plate is also uniform. In dual-passive forming, the minimum thickness is 0.0971 mm and 0.0974 mm, accounting for 97.1% and 97.4% of the initial thickness, respectively. Because the plate is subjected to less stress, the plastic deformation is relatively less, so the plate is not very thin in double passive deformation. Overall, the remaining thickness of all plates is above 85%. It is shown that the thickness distribution of sheet metal formed by rubber pad forming is relatively uniform. In industrial operations, there is a low probability of stress concentration.

4.4 Metallographic experiment

In addition, as shown in Fig. 16, a metallographic microscope is used, and metallographic photographs of the 304 stainless steel sheet are displayed. Picric acid hydrochloride alcohol solution (1 g picric acid + 5 mL hydrochloric acid + 100 mL alcohol) is used as a corrosive agent. The microstructure of SS304 plate before forming is austenite coarse-grained structure with uniform distribution. The microstructure is uniform

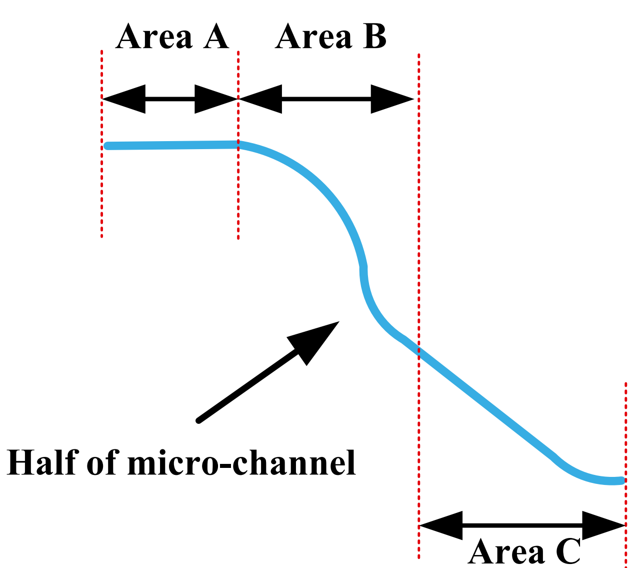

Fig. 14 Sheet thickness in three areas of two-step micro-channel

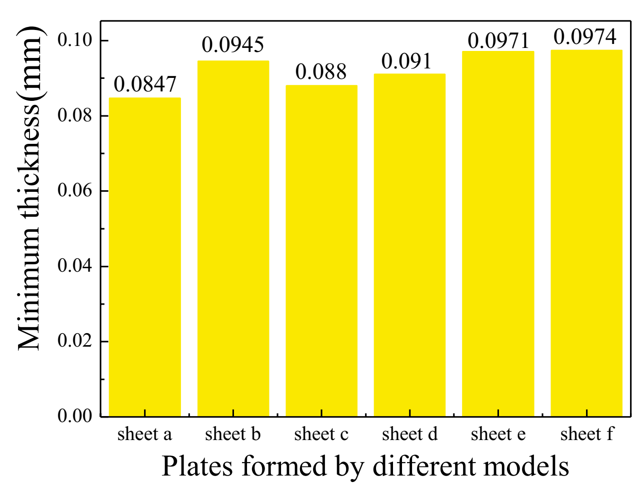

Fig. 15 Minimum thickness of each plate

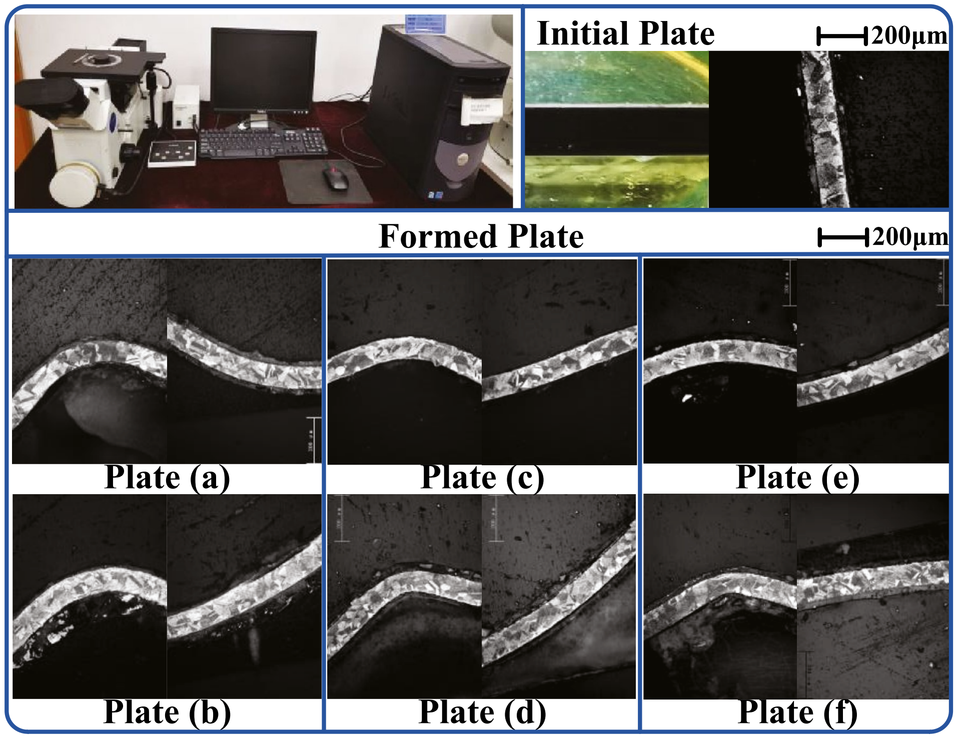

Fig. 16 Metallographic photograph of stainless steel 304

equiaxed grain with a few annealing twins. The microscopic metallographic pictures of SS304 after forming are shown in figure. Two positions are selected for each formed plate, the ridge and the top. Compared with the structure before forming, there is a serious plastic deformation on the SS304 sheet, thus presenting a different structure. The grain is elongated along the stamping direction and becomes finer. There are defects at grain boundaries, and dislocation density is increased. The grain sizes of the sheets formed by the double passive forming method are slightly larger than that of other plates due to less stress.

5 Conclusions

In this study, by means of finite element simulation and deep drawing experiment, rubber pad forming process was used to form metal sheet with two-step micro-channel, and the possibility of forming two plates at the same time was discussed. A new rubber pad forming method for multilayer thin plate is presented, which can obviously improve the forming efficiency. In this study, convex molds were used to produce plates, and the micro-channels were obtained according to the design shape. The shapes of micro-channels formed by different models are compared with that of ideal micro-channels. It is shown that this method has high forming precision and can improve forming efficiency significantly.

Results:

1. The rubber pad forming process was studied by means of finite element simulation and deep drawing experiment, and the active forming process and passive forming process were proposed. It was found that both of them could be used to manufacture the two-step micro-channel metal sheet.
2. In this paper, a method of forming two metal sheets simultaneously by rubber pad forming process is put forward. Through contrast experiment, it is found that active and passive mixed forming method can be used to form two plates precisely at the same time, which greatly improves the forming efficiency.
3. Less stress is transferred to the plate by passive forming. So the more layers of the plate, the greater the required forming force, and forming is more difficult. The conclusion of this paper will lay a solid theoretical foundation for further research on the simultaneous forming of 4 or more layers of metal sheets.

Author contribution F. Teng: Finite element simulation, forming experiment, writing (original draft), and writing (review and editing). H.Y. Wang: Supervision, provide idea, funding acquisition, and writing (review and editing). S.N. Shi: Finite element simulation and forming experiment. L. Jiang: Finite element simulation and forming experiment. J.C. Sun: Supervision and funding acquisition. J. Sun: Provide advice and writing (review and editing). H.S. Di: Provide advice and writing (review and editing). S.H. Zhang: Provide advice and writing (review and editing).

Funding This work is financially supported by the National Natural Science Foundation of China (No. 51905068), the Natural Science Foundation of Liaoning Province (No. 2020-HYLH-24), and the open research fund from the State Key Laboratory of Rolling and Automation, Northeastern University (No. 2020RALKFKT012).

Data availability The datasets generated and/or analyzed during the current study are available from the corresponding author on reasonable request.

Declarations

Ethical approval This article does not contain any studies with human participants or animals performed by any of the authors.

Consent to participate Applicable.

Consent to publish Applicable.

Conflict of interest The authors declare no competing interests.

Informed consent All the authors listed have approved the manuscript that is enclosed.

References

1. Huang BH, Li HW, Xia SZ, Xu TT (2020) Experimental investigation of the flow and heat transfer performance in micro-channel heat exchangers with cavities. Int J Heat Mass Tran 159:1–10
2. Belhassen L, Koubaa S, Wali M, Dammak F (2016) Numerical prediction of springback and ductile damage in rubber-pad forming process of aluminum sheet metal. Int J Mech Sci 117:218–226
3. Ramezani M, Ripin ZM, Ahmad R (2009) Computer aided modelling of friction in rubber-pad forming process. J Mater Process Tech 209(10):4925–4934
4. Elyasi M, Khatir FA, Hosseinzadeh M (2017) Manufacturing metallic bipolar plate fuel cells through rubber pad forming process. Int J Adv Manuf Tech 89(9–12):3257–3269
5. Kolandooz R, Asghari S, Rashid-nadimi S, Amirfazli A (2017) Integration of finite element analysis and design of experiment for the investigation of critical factors in rubber pad forming of metallic bipolar plates for PEM fuel cells. Int J Hydrogen Energ 42:575–589
6. Timurkutluk B, Onbilgin S (2020) Design and fabrication of novel interconnectors for solid oxide fuel cells via rubber pad forming. Int J Energ Res 44(11):8716–8729
7. Lee J, Park H, Kim SJ, Kwon YN, Kim D (2017) Numerical investigation into plastic deformation and failure in aluminum alloy sheet rubber-diaphragm forming. Int J Mech Sci 142:112–120
8. Wang CJ, Wang HY, Chen G, Zhu Q, Zhang GW, Cui LJ, Zhang P (2020) Size effects affected uniaxial tensile properties and formability in rubber pad microforming process of pure nickel thin sheets. Int J Mech Sci 182:105757
9. Gau JT, Gu H, Liu XH, Huang KM, Lin BT (2015) Forming micro channels on aluminum foils by using flexible die forming process. J Mater Process Tech 19:102–111
10. Wang HY, Wei Z, Teng F, Zhang PC, Sun JC, Ji SJ (2019) Numerical simulation and experiment research on forming of two-step channel based on rubber pad pressing. Int J Adv Manuf Tech 101(5–8):2175–2189
11. Wang HY, Teng F, Wei Z, Zhang PC, Sun JC, Ji SJ (2019) Simulation research about rubber pad forming of corner channel with convex or concave mould. J Maunf Process 40:94–104
12. Jin CK, Jeong MG, Kang CG (2014) Effect of rubber forming process parameters on micro-patterning of thin metallic plates. Procedia Eng 81:1439–1444
13. Hossein TG, Majid E, Mohammad JM (2020) Investigation of failure during rubber pad forming of metallic bipolar plates. Thin Wall Struct 150:106671
14. Hao XH, Peng B, Xie G, Chen Y (2016) Efficient on-chip hotspot removal combined solution of thermoelectric cooler and minichannel heat sink. Appl Therm Eng 100:170–178
15. Fukagata K, Kasagi N, Koumoutsakos P (2006) A theoretical prediction of friction drag reduction in turbulent flow by superhydrophobic surfaces. Phys Fluids 18(5):051703
16. Ou J, Perot B, Rothstein JP (2004) Laminar drag reduction in microchannels using ultrahydrophobic surfaces. Phys Fluids 16(12):4635–4643
17. Chen T, Ye J (2013) Fabrication of micro-channel arrays on thin stainless steel sheets for proton exchange membrane fuel cells using micro-stamping technology. Int J Adv Manuf Tech 64(9–12):1365–1372
18. Li WK, Zhang QL, Wang C, Yan XH, Shen SY, Xia GF, Zhu FJ, Zhang JL (2017) Experimental and numerical analysis of a three-dimensional flow field for PEMFCs. Appl Energ 195:278–288
19. Teng F, Wang HY, Sun JC, Kong XW, Sun J, Zhang SH (2021) Thickness analysis of complex two-step micro-groove on plate during rubber pad forming process. P I Mech Eng C-J MEC 235(1):122–135
20. Liu YX, Hua L (2010) Fabrication of metallic bipolar plate for proton exchange membrane fuel cells by rubber pad forming. J Power Sources 195(11):3529–3535
21. Liu YX, Hua L, Lan J, Wei X (2010) Studies of the deformation styles of the rubber-pad forming process used for manufacturing metallic bipolar plates. J Power Sources 195:8177–8184
22. Peng LF, Hu P, Lai XM, Mei DQ, Ni J (2009) Investigation of micro/meso sheet soft punch stamping process—simulation and experiments. Mater Design 30:783–790
23. Peng LF, Liu DA, Hu P, Lai XM, Ni J (2010) Fabrication of metallic bipolar plates for proton exchange membrane fuel cell by flexible forming process-numerical simulations and experiments. J Fuel Cell Sci Tech 73:299–302
24. Jin CK, Lee KH, Kang CG (2015) Performance and characteristics of titanium nitride, chromium nitride, multi-coated stainless steel 304 bipolar plates fabricated through a rubber forming process. Int J Hydrogen Energ 40(20):6681–6688